光学学报

基于扫描振镜的超短脉冲激光旋切制孔光学系统设计

张健，卓瑾，金会良，刘虹君，樊非，张清华，许乔*
中国工程物理研究院激光聚变研究中心，四川 绵阳 621900

摘要 在电子产业、航空航天、医药、汽车、微机电器件等领域，精密微孔是器件、功能部件上的重要结构单元。当前超短脉冲激光精密微孔制备缺乏高稳定、体积小、低成本的旋切加工系统。针对一百到几百微米尺寸的精密微孔加工需求，设计了一种基于扫描振镜的超短脉冲激光旋切制孔光学系统，并对系统的反射像和公差进行了分析。通过采用摄远结构设计和对称设计，大幅缩短了系统镜头总长，设计结果为加工孔径范围100～400 μm，最大加工深径比10∶1。搭建了基于扫描振镜的超短脉冲激光旋切制孔光学系统，对制孔效果进行了实验验证，制孔结果显示，基于扫描振镜的超短脉冲激光旋切制孔光学系统能实现高精度的微孔制备。

关键词 超短脉冲激光；旋切制孔；微孔；镜头；摄远结构；公差分析
中图分类号 O439 **文献标志码** A **DOI：** 10.3788/AOS230521

1 引 言

随着电子产业、航空航天、医药、汽车、微机电器件等行业的发展，对器件、结构的小型化和功能结构提出了新的要求，其中100 μm至亚毫米尺寸精密微孔是重要的结构单元，这些孔的加工已经成为当前这些行业发展的焦点[1-4]。其发展趋势是小尺寸、大深径比、加工精度高、加工效率高、无热效应、无微裂纹、无重铸层等[5]。传统的加工方法，例如机械刀具、水刀、超声加工等都面临加工精度不足或刀具磨损等问题[6-7]。电火花属于电加工技术，适用于金属等导电性良好的材料，但无法加工非导电的材料[8]，存在热效应和微裂纹等问题。而长脉冲激光加工技术由于其热效应强、加工质量差，产生了明显的热影响区、重铸层和微裂纹，无法满足高质量微孔加工的要求[9-11]。上述加工方法已不适用于小尺寸孔结构加工发展的需求。由超短脉冲激光产生的光场经过聚焦后，光强可以达到10^{15} W/cm^{2}以上，超过介质内部的库仑场强，多光子效应和量子隧穿效应开始凸显。对于金属和陶瓷等材料，飞秒聚焦光场可将材料直接电离形成等离子体[12]。同时，由于其与材料作用时间在几皮秒(ps)及以下，因此超短脉冲激光被视为无材料选择性的“冷加工”方式[13-14]。尤其是近年来啁啾脉冲放大、全固态飞秒、光纤飞秒等技术不断发展，飞秒激光器在高重复频率、高功率、稳定性和实用性等方面得到了迅速的发展[15-18]。因此，飞秒激光加工具备较高的材料去除率和更加广泛的应用范围，不再仅适用于微纳加工和实验室研究使用。尤其是将高速扫描振镜技术、光楔旋切加工技术、空间光调制器等高速扫描加工技术与高功率飞秒激光的加工能力结合，飞秒激光加工具有实现大材料去除量的批量化高效加工能力。鉴于此，超短脉冲激光成为微孔加工极具前景的加工技术[19]。

2 旋切制孔光学系统原理

目前国际上主流的长直孔、倒锥孔加工方法采用光楔和道威棱镜旋转来实现，这种螺旋线扫描方法称为旋切制孔[20-21]，基本原理是通过镜组的高速旋转和光学器件折射、偏转实现螺旋线扫描，结合道威棱镜实现光束沿光轴的旋转，对光束匀化，然后通过聚焦镜对光束聚焦，最终完成精密孔的加工。在此基础上，出现了双光楔、三光楔、四光楔等不同方案[22]，这些系统在光学设计上是在聚焦镜组前产生带有离轴角度的平行光，不同方向的离轴平行光束通过聚焦镜组后先会聚再离轴聚焦，光束会聚部分的直径小于等于加工的孔径，并且聚焦激光束与加工孔前表面成锐角，避免了孔口挡光，减小了热效应，图1为旋切制孔系统聚焦光场分布，旋切制孔可以实现陡直孔、锥孔、腰形孔等不同回转体的孔形加工，加工孔壁粗糙度低、无毛刺，加工深径比可达到15以上。因此，旋切制孔能实现高精度、高质量、高深径比的微孔加工。

收稿日期：2023-02-06；**修回日期**：2023-02-26；**录用日期**：2023-04-10；**网络首发日期**：2023-05-08
通信作者：*xuq_rclf@163.com

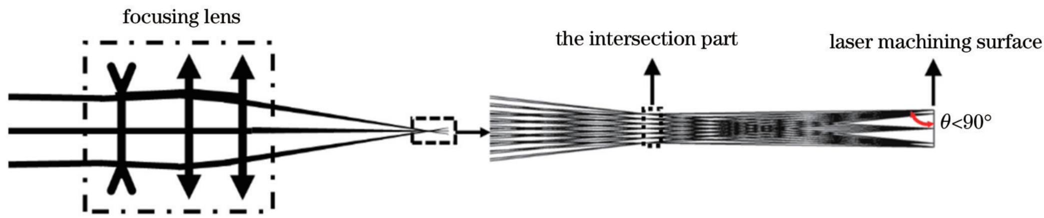

图1 旋切制孔系统聚焦光场分布

Fig. 1 Distribution of the focusing light field of helical laser drilling system

基于上述旋切制孔光学原理，最近几年也发展了基于旋转柱面透镜旋切扫描装置[23]、基于三反射系统的旋切扫描装置[24]、基于平行平板扫描头的旋切扫描装置[25]、振镜结合4f光学系统的旋切扫描装置[26]等精密微孔加工方法。目前基于光楔旋转的加工方法需要镜组的高速旋转（≥3000 r/min），多光楔也会导致旋转组件尺寸较大，对旋转机械系统的精度要求极高，整体造价昂贵。对于100 μm左右的精密孔加工，旋转轴微小的轴跳就可能导致加工偏差，并且这种加工方法只能加工陡直圆孔或倒锥孔、腰形孔等回转体，无法实现异形孔的加工（例如方形孔、簸箕形孔）。基于三反射系统的旋切扫描装置需要3个反射镜的精密同步控制和复杂的控制算法，实现难度较高。常规的振镜结合4f光学系统的旋切扫描加工方法通过XY方向两个反射镜的运动实现扫描，精度主要受限于振镜的扫描角分辨率。为实现几十微米精密孔加工，常需要光束大的离轴量，而采用常规的镜组对光束进行离轴，离轴量小，聚焦镜组光束会聚处的直径大，难以加工100 μm左右精密孔，并且光路较长，系统整体尺寸大，微小的光束指向性偏移可能导致加工精度的下降，对激光器的指向性和使用环境要求高。因此，目前缺乏高稳定、体积小、低成本，以及可加工一百至几百微米精密孔的旋切加工系统。

为实现一百到几百微米尺寸的精密微孔加工，本文设计了一种微孔旋切扫描加工光学系统，通过振镜和旋切加工镜头实现精密微孔加工和异形孔的加工，孔径范围为100～400 μm。振镜实现任意光束轨迹扫描，通过旋切加工镜头在加工面产生先会聚再离轴聚焦的光束走向。旋切加工镜头采用摄远结构设计和对称设计，大幅缩短了系统镜头总长，增加了聚焦激光束的离轴角度。整个系统无高速旋转部件，避免了轴跳可能导致的加工偏差，振镜为成熟的器件，控制实现容易，能实现陡直孔、锥形孔和异形孔等孔形的加工。

为实现精密微孔加工，要求聚焦镜组后光束会聚部分的直径小于等于加工的孔径，并且要求聚焦激光光轴与加工孔前表面成锐角。为实现这两个要求，本文旋切加工镜头由扫描镜组、传像镜组和聚焦镜组组成，旋切加工镜头焦距f表示为

$$f=f_3\times f_1/f_2\ , \tag{1}$$

式中：f_1为扫描镜组焦距为；f_2为传像镜组焦距；f_3为聚焦镜组焦距。为了实现系统高稳定和小型化的目标，本文将扫描镜组和传像镜组设计为摄远型镜头结构。摄远型镜头结构在保持焦距不变的同时缩短了镜头光学距离总长，即镜头光学距离总长小于焦距，同时增加了离轴光束的离轴角，有利于在聚焦镜组后端产生更小的光束会聚部分直径。图2为旋切加工镜头的结构示意图，摄远型镜头结构由前正透镜组和后负透镜组组成。为了实现较好的聚焦质量，设计时通过增加透镜数量来分摊光焦度，扫描镜组由两个正透镜和一个负透镜组成，传像镜组与扫描镜组采用对称结构设计。本文通过控制摄远比h（镜头焦距/镜头光学距离总长）来控制光束会聚部分的直径，从而达到最小加工直径的要求。为了增加旋切加工镜头的工作距，聚焦镜组采用反摄远结构，即负透镜在前、正透镜在后，并通过光学设计软件优化得到最佳的聚焦效果。

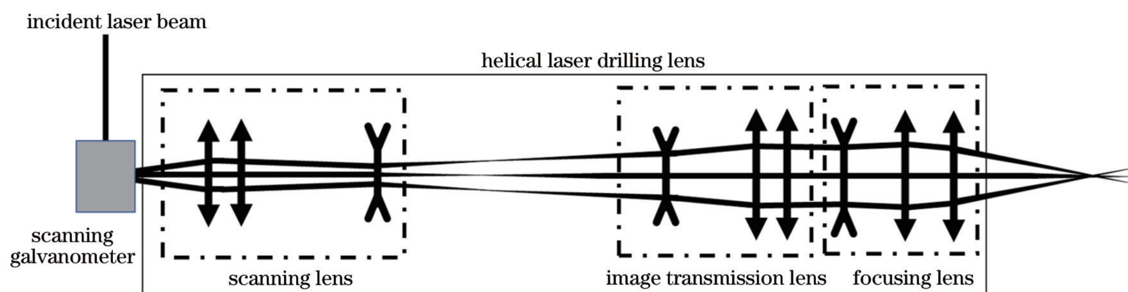

图2 旋切加工镜头初始结构示意图

Fig. 2 Schematic diagram of the initial structure of helical laser drilling lens

3 系统设计与分析

3.1 旋切加工镜头光学系统设计要求

超短脉冲激光中心波长为 515 nm，光谱范围（半峰全宽）为 510～520 nm，脉冲宽度为 500 fs，准直光斑直径为 4 mm，光束质量 M^2=1.2。本文的设计目标为最小加工孔径 100 μm，最大加工深度 1000 μm，即加工的深径比为 1000/100=10。对于微孔加工，一般要求聚焦光斑直径小于 1/4 最小加工孔径。根据加工深径比的要求，确定旋切加工镜头 F#=10（镜头焦距/入射光束直径），入射光束直径为 4 mm，得到旋切加工镜头焦距 f=100 mm。聚焦光斑直径 D 的计算公式为

$$D = M^2 \times 2.44\lambda \times F \text{，} \tag{2}$$

式中：λ 为激光中心波长，计算得到聚焦焦斑直径为 15 μm，满足聚焦光斑直径小于 1/4 最小加工孔径的要求。综上所述，旋切制孔光学系统设计参数如表 1 所示。

表 1　旋切制孔光学系统设计指标

Table 1　Design specifications of helical laser drilling system

System parameter	Design specification
Wavelength /nm	510-520
Pulse duration /fs	500
Beam quality M^2	1.2
Focal length /mm	40
F number	10
Working distance /mm	≥30
Focal spot diameter /μm	15
Processing hole aperture range /μm	100-400
Wave aberration (RMS, 515 nm)	≤0.05λ
Total length /mm	≤520

3.2 旋切加工镜头光学系统设计

通过 ZEMAX 光学设计软件开展光学系统设计，对于高功率超短脉冲，旋切制孔光学系统从像质上需要考虑消色差和最佳的聚焦效果，从系统性能上需要考虑脉冲色散展宽、元件低热膨胀、元件损伤阈值和元件反射像等问题。激光脉冲光谱带宽为 10 nm，设计时正透镜选择阿贝数较高的材料，减小脉冲色散展宽，同时满足高损伤阈值、低热膨胀要求，最终选择熔石英 JGS1 玻璃。负透镜选择成都光明公司重火石玻璃（牌号 H-ZF13），正负透镜组合消除色差。根据旋切加工镜头焦距计算公式 $f=f_3 \times f_1/f_2$，结合系统排布要求和加工参数要求，确定 f_1=400 mm，f_2=500 mm，f_3=50 mm。根据计算参数、选择的材料，以及摄远型镜头、反摄远型镜头排布来设置各个镜组的初始结构，确定光学结构形式和外形尺寸，并在此基础上建立约束条件对各个镜组进行优化，其中扫描镜组和传像镜组设置摄远比 $h \geq 2$。镜组优化完成后，将镜组组合，进行联合优化，直至最终系统波像差和各项指标满足要求。然后对系统反射像和公差进行分析，根据实际情况对设计进行微调。最终设计结果如图 3 所示，其中扫描镜组摄远比 h_1=2，传像镜组摄远比 h_2=2.1，系统总长为 512.5 mm（第一个透镜前表面到加工面），远小于三个镜组焦距之和 950 mm（$f_1+f_2+f_3$），即本文设计的光学系统总长为未采用摄远结构总长的 0.54。图 4 为聚焦光场设计结果的放大图像，光束会聚处的直径为 86 μm，聚焦光场 F#=10，因此本方案具备实

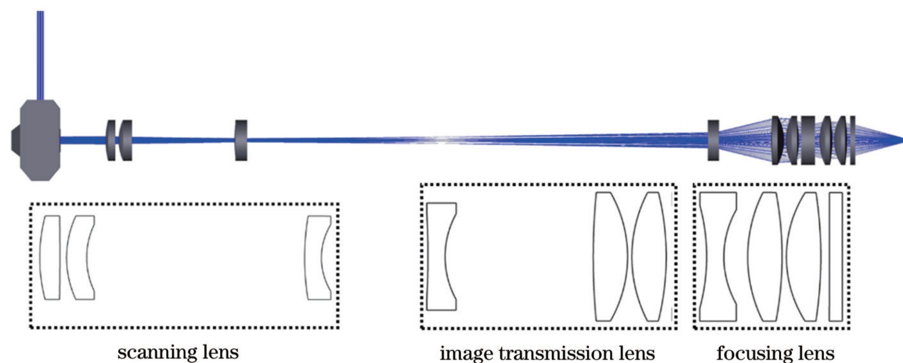

图 3　旋切加工镜头设计结果

Fig. 3　Design result of the helical laser drilling lens

现最小孔径 100 μm、最大深径比 10:1 的加工能力。系统工作距 35 mm，满足设计要求。

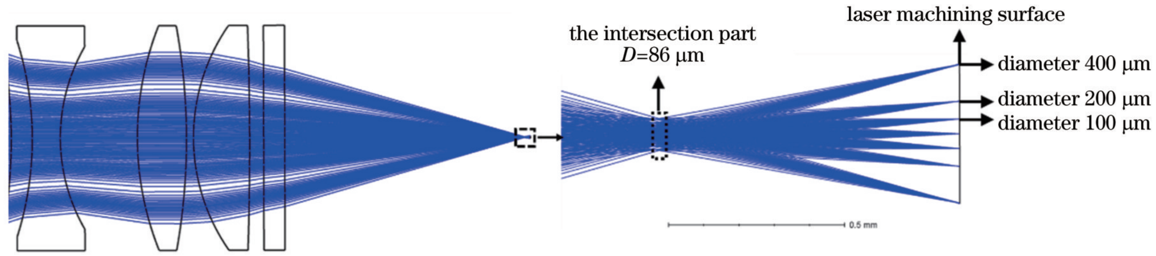

图 4 旋切加工镜头聚焦光场设计结果

Fig. 4 Design results of the focusing light field for helical laser drilling lens

图 5 为聚焦光场点列图和波像差结果，点列图和波像差是反映光学系统聚焦能力的重要指标，孔径在 100～400 μm 范围内，点列图结果显示所有聚焦焦点都在艾里斑轮廓内，波像差(RMS，515 nm)最大为 0.02λ，设计结果表明，旋切加工镜头达到了衍射极限的聚焦能力。

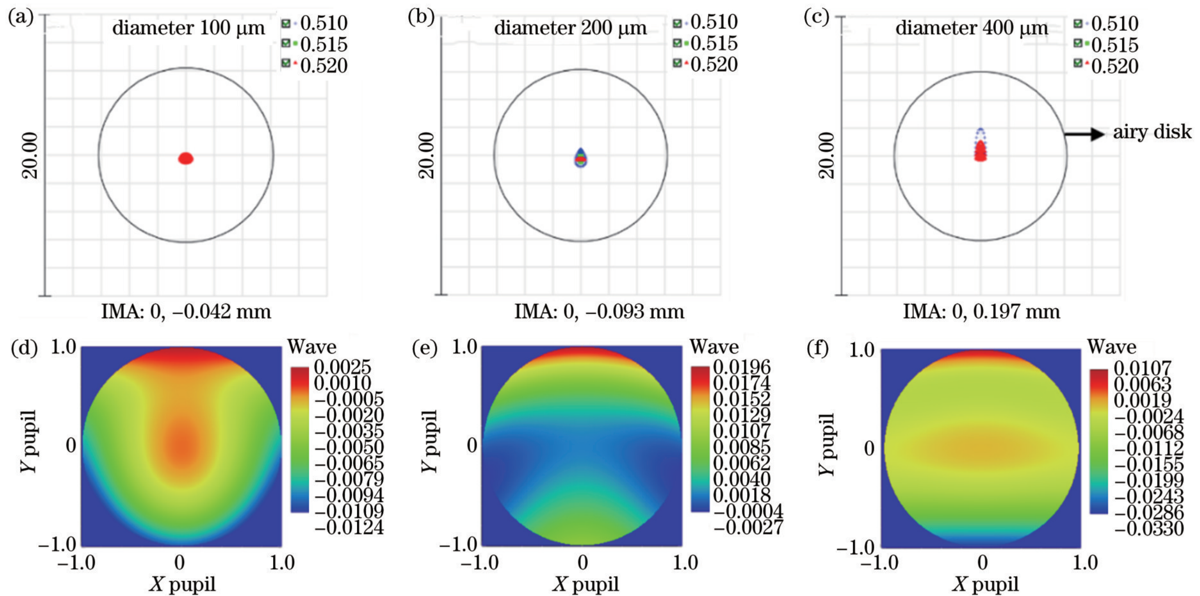

图 5 孔径分别为 100 μm、200 μm、400 μm 时，旋切加工镜头聚焦光场点列图和波像差结果。(a)～(c)点列图；(d)～(f)波像差

Fig. 5 Spot diagrams and wave aberration results of focusing light field for helical laser drilling lens, when diameter is 100 μm, 200 μm, and 400 μm, respectively. (a)–(c) Spot diagrams; (d)–(f) wave aberration results

3.3 旋切加工镜头反射像分析

在高功率以及高峰值功率应用场合，光学元件表面的残余反射光聚焦(反射像)具有极高的能量，可能导致元件内部材料或膜层的损伤。因此在设计镜头时，需要调节元件的曲率半径、间隔等参数，让元件避开残余反射光聚焦处。本文设计的旋切加工镜头属于高峰值功率应用场合，在设计时对反射像进行了分析，其中扫描镜组元件主要为凸凹结构，不产生有害的反射像。传像镜组和聚焦镜组主要为双凸和双凹元件，存在确定的反射像，图 6 所示为传像镜组和聚焦镜组所有反射像的位置，以传像镜组的第 1 个元件的第 1 面为坐标原点，所有面依次进行编号，第 4、6、7、10、12 面存在反射像，都不在元件内部或表面。因此，本文设计的旋切加工镜头产生的反射像不会对元件内部材料和表面膜层产生损伤。

3.4 旋切加工镜头公差分析

旋切加工镜头光学透镜数量较多，透镜加工或安装所引起的光束偏移或波像差变化可能对激光加工聚焦产生较大的影响。为使本文的设计方案满足实际加工、生产的需求，有必要对系统进行公差分析。根据当前光机系统加工、装调的能力，对系统进行公差分配，部分公差分配如表 2 所示，对旋切加工镜头的光学元件依次进行编号，并分配公差值。以光斑半径(RMS)作为评价标准，采用蒙特卡罗方法对所有元件公差进行综合分析，共进行了 200 次分析计算，最大半径变化为 2.2 μm，90% 的情况半径变化小于 1.3 μm，远小于聚焦艾里斑直径 15 μm。结果表明，在本文的公差分配范围内，旋切加工镜头成像质量良好，满足使用

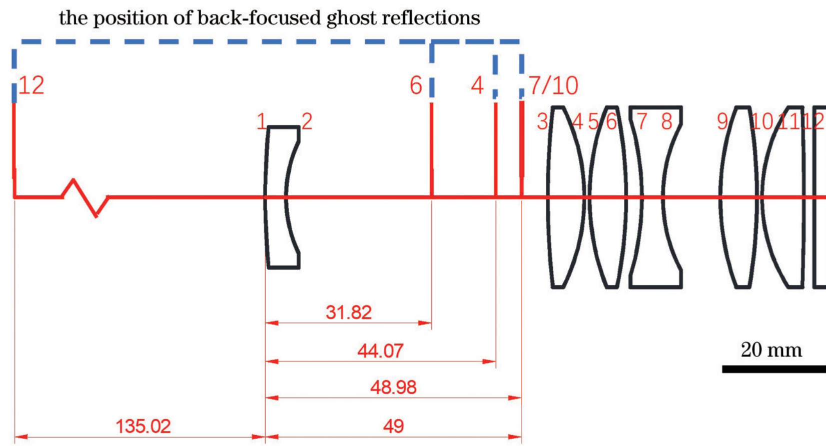

图 6 旋切加工镜头反射像分析

Fig. 6 Analysis of back-focused ghost reflections of helical laser drilling lens

表 2 旋切制孔光学系统公差分析

Table 2 Tolerance analysis of helical laser drilling system

Lens number		Machining tolerance			Assembly tolerance		
		Fringes / irregularity	Thickness /mm	Surface decenter /μm	Element tilt /(′)	Element decenter /μm	Air space /mm
Lens 1	Front surface	3/0.3	±0.05	20	4	15	±0.05
	Rear surface	3/0.3		20			
Lens 2	Front surface	3/0.3	±0.05	20	4	15	±0.05
	Rear surface	3/0.3		20			
Lens 3	Front surface	3/0.3	±0.05	20	4	15	±0.05
	Rear surface	2/0.2		10			
Lens 4	Front surface	2/0.2	±0.05	20	4	15	±0.05
	Rear surface	2/0.2		10			
Lens 5	Front surface	2/0.2	±0.05	20	3	15	±0.05
	Rear surface	2/0.2		10			
Lens 6	Front surface	2/0.2	±0.05	10	3	15	±0.05
	Rear surface	2/0.2		20			
Lens 7	Front surface	2/0.2	±0.05	20	3	15	±0.05
	Rear surface	2/0.2		10			
Lens 8	Front surface	3/0.3	±0.05	20	3	15	±0.05
	Rear surface	3/0.3		20			
Lens9	Front surface	2/0.2	±0.05	10	3	15	±0.05
	Rear surface	2/0.2		20			

要求。

3.5 旋切制孔光学系统实验分析

根据设计结果，对旋切加工镜头进行了加工和装配，并对基于扫描振镜的超短脉冲激光旋切制孔光学系统进行了组装。采用超短脉冲激光，对钛合金和钛金属进行了制孔实验，制孔孔径分别设置为 0.25 mm 和 0.4 mm，样品厚度为 2 mm。采用激光共聚焦显微镜对制孔结果进行了测量，结果如图 7 所示。加工孔径与设置值偏差小于 10 μm，前孔和背孔空间偏差小于 10 μm，制孔圆度（孔径短轴/长轴）优于 98%。制孔结果显示，基于扫描振镜的超短脉冲激光旋切制孔光学系统能实现高精度的微孔制备。

4 结 论

针对一百到几百微米尺寸的精密微孔加工要求，本文设计了一种基于扫描振镜的超短脉冲激光旋切制孔光学系统，其中旋切加工镜头采用了摄远结构设计和对称结构设计，将镜头总长缩短到了 512.5 mm，所设计的加工孔径范围为 100～400 μm，最大加工深径比为 10:1。对旋切加工镜头进行了反射像分析和公

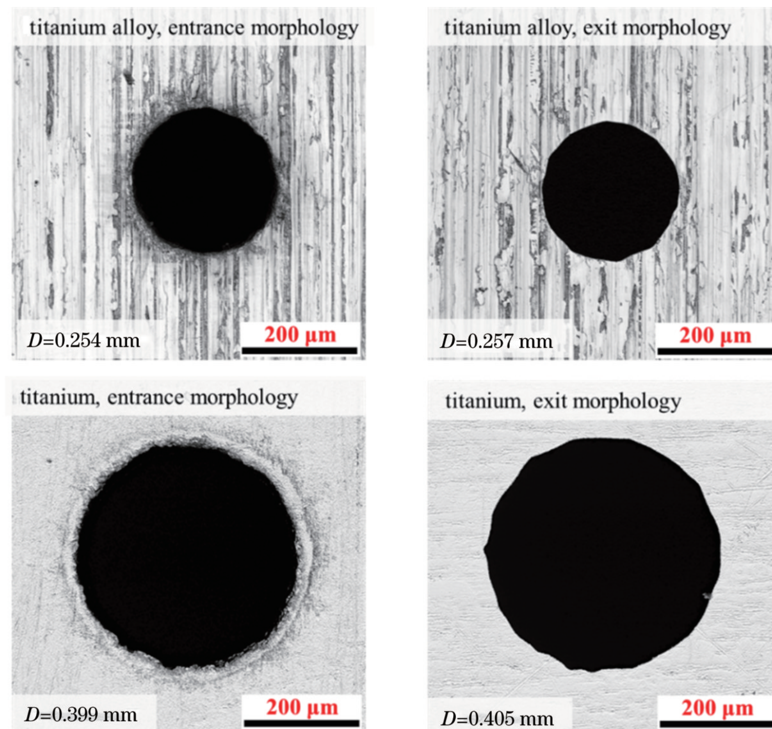

图7　旋切制孔光学系统的制孔结果

Fig. 7　Images of micro-holes processed by helical laser drilling system

差分析,结果表明,设计结果无有害反射像,公差满足实际装配要求,成像质量良好。本文搭建了基于扫描振镜的超短脉冲激光旋切制孔光学系统,对制孔效果进行了实验验证,制孔结果显示,基于扫描振镜的超短脉冲激光旋切制孔光学系统能实现高精度的微孔制备。所设计的旋切制孔光学系统具有高稳定、体积小、低成本的优势,为超短脉冲激光精密微孔制备提供了一种可选的方案。

参　考　文　献

[1] Zhang L, Huang H. Micro machining of bulk metallic glasses: a review[J]. The International Journal of Advanced Manufacturing Technology, 2019, 100(1): 637-661.

[2] 任云鹏, 程力, 周王凡, 等. 铝合金飞秒激光单步法和三步法旋切打孔技术研究[J]. 中国激光, 2022, 49(22): 2202020.
Ren Y P, Cheng L, Zhou W F, et al. Study on one-step and three-step rotary cutting drilling technology of aluminum alloy by femtosecond laser[J]. Chinese Journal of Lasers, 2022, 49(22): 2202020.

[3] Hasan M, Zhao J W, Jiang Z Y. A review of modern advancements in micro drilling techniques[J]. Journal of Manufacturing Processes, 2017, 29: 343-375.

[4] Chen Y H, Li Z C, Cao H, et al. Determination of laser entrance hole size for ignition-scale octahedral spherical hohlraums[J]. Matter and Radiation at Extremes, 2022, 7(6): 065901.

[5] 王锋, 罗建军, 李明. 飞秒激光高精细加工柴油机喷油嘴倒锥孔法[J]. 光子学报, 2014, 43(4): 0414003.
Wang F, Luo J J, Li M. High-precision method of machining taper holes of diesel engine nozzle with femtosecond laser[J]. Acta Photonica Sinica, 2014, 43(4): 0414003.

[6] Liu Y, Quan Y, Wu C J, et al. Single diamond scribing of SiC_f/SiC composite: force and material removal mechanism study[J]. Ceramics International, 2021, 47(19): 27702-27709.

[7] Zhang B, Du Y N, Liu H L, et al. Experimental study on high-speed milling of SiCf/SiC composites with PCD and CVD diamond tools[J]. Materials, 2021, 14(13): 3470.

[8] Diaz O G, Luna G G, Liao Z R, et al. The new challenges of machining ceramic matrix composites (CMCs): review of surface integrity[J]. International Journal of Machine Tools and Manufacture, 2019, 139: 24-36.

[9] Whitlow T, Pitz J, Pierce J, et al. Thermal-mechanical behavior of a SiC/SiC CMC subjected to laser heating[J]. Composite Structures, 2019, 210: 179-188.

[10] Wang J, Cheng L F, Liu Y S, et al. Enhanced densification and mechanical properties of carbon fiber reinforced silicon carbide matrix composites via laser machining aided chemical vapor infiltration[J]. Ceramics International, 2017, 43(14): 11538-11541.

[11] 张云龙, 孙树峰, 王茜, 等. 激光加工微孔质量的研究[J]. 激光与光电子学进展, 2021, 58(19): 1900002.
Zhang Y L, Sun S F, Wang X, et al. Research on quality of micro-holes fabricated by laser drilling[J]. Laser & Optoelectronics Progress, 2021, 58(19): 1900002.

[12] Stoian R, Colombier J P. Advances in ultrafast laser structuring of materials at the nanoscale[J]. Nanophotonics, 2020, 9(16): 4665-4688.

[13] Malinauskas M, Žukauskas A, Hasegawa S, et al. Ultrafast laser processing of materials: from science to industry[J]. Light: Science & Applications, 2016, 5(8): 16133.

[14] Wang X D, Yu H B, Li P W, et al. Femtosecond laser-based processing methods and their applications in optical device manufacturing: a review[J]. Optics & Laser Technology, 2021, 135: 106687.

[15] Lopez J, Mishchik K, Mincuzzi G, et al. Efficient metal processing using high average power ultrafast laser[J]. Journal of Laser Micro, 2017, 12(3): 296-303.

[16] Mans T, Dolkemeyer J, Schnitzler C. High power femtosecond lasers: efficient power scaling of ultrashort pulse lasers to kW

range and more[J]. Laser Technik Journal, 2014, 11(3): 40-43.

[17] Gronloh B, Russbueldt P, Jungbluth B, et al. Green sub-ps laser exceeding 400 W of average power[J]. Proceedings of SPIE, 2014, 8959: 89590T.

[18] Limpert J, Roser F, Schreiber T, et al. High-power ultrafast fiber laser systems[J]. IEEE Journal of Selected Topics in Quantum Electronics, 2006, 12(2): 233-244.

[19] Jia X S, Chen Y Q, Liu L, et al. Advances in laser drilling of structural ceramics[J]. Nanomaterials, 2022, 12(2): 230.

[20] Zibner F, Fornaroli C, Holtkamp J, et al. 1μm adjustment-tolerance for high-precision helical laser drilling[J]. Proceedings of SPIE, 2015, 9582: 95820C.

[21] Fornaroli C, Holtkamp J, Gillner A. Laser-beam helical drilling of high quality micro holes[C]//International Congress on Applications of Lasers & Electro-Optics, AIP Publishing, 2012: 1040-1045.

[22] 阿占文, 陈灵灵, 吴影, 等. 超快激光旋光钻孔孔径和锥度的控制[J]. 中国激光, 2021, 48(8): 0802017.
A Z W, Chen L L, Wu Y, et al. Controlling of diameter and taper in ultrafast laser helical drilling[J]. Chinese Journal of Lasers, 2021, 48(8): 0802017.

[23] Lendner F. Smart ultra short pulse laser processing with rotating beam: laser micro drilling, cutting, and turning[J]. Proceedings of SPIE, 2020, 11268: 112681Z.

[24] 孙喜博, 张颖, 马文静, 等. 一种多轴旋切扫描系统的使用方法: CN114505602B[P]. 2022-07-01.
Sun X B, Zhang Y, Ma W J, et al. Multi-axis rotary-cut scanning system and use method thereof: CN114505602B[P]. 2022-07-01.

[25] 黄江波, 李一凡, 朱文宇. 异形气膜孔的激光加工方法: CN110026677A[P]. 2020-05-19.
Huang J B, Li Y F, Zhu W Y. Laser processing method for irregular gas film holes: CN110026677A[P]. 2020-05-19.

[26] 王建刚, 王雪辉, 温彬, 等. 用于旋切打孔的光学装置: CN106392310B[P]. 2019-06-11.
Wang J G, Wang X H, Wen B, et al. Optical device for rotary cutting and punching: CN106392310B[P]. 2019-06-11.

Optical Design of Helical Drilling System with Ultrashort Pulse Laser Based on Scanning Galvanometer

Zhang Jian, Zhuo Jin, Jin Huiliang, Liu Hongjun, Fan Fei, Zhang Qinghua, Xu Qiao*

Laser Fusion Research Center, China Academy of Engineering Physics, Mianyang 621900, *Sichuan, China*

Abstract

Objective In the electronic industry, aerospace, medicine, automobile, and micro-electro-mechanical system, micro-holes are important structural units of devices and functional parts. The current development trend of micro-hole processing is small size, high aspect ratio, high machining accuracy, high machining efficiency, no recast layer, no heat-affected zone, and no micro cracks. At present, several methods, such as mechanical, electro-discharge, electrochemical, and pulse laser drilling, are used for micro-hole machining. Ultrashort pulse laser processing is particularly versatile and can guarantee a high level of controlling the process due to the ultrashort time scale and ultra-high peak power density characteristics. It has been used for micro-hole drilling with limited heat-affected zone to provide high quality and precision, especially for hard and brittle materials. If the ultrashort pulse laser is used as a drilling tool, the beam must be rotated in a circular movement. At present, helical laser drilling technology is mainly based on the rotation of optical components, such as Dove prism, wedge plates, and cylindrical lenses. However, there is still a lack of high stability, small size, and low-cost laser drilling system. In this paper, a helical laser drilling system based on a scanning galvanometer is designed to meet the requirements of precise micro-hole drilling with a diameter ranging from 100 μm to a few hundred microns.

Methods The ultrashort pulse laser drilling system is based on a scanning galvanometer and a helical laser drilling lens. The scanning galvanometer can be rotated in XY direction with high accuracy and high speed. The helical laser drilling lens is made up of a scanning lens, an image transmission lens, and a focusing lens. The basic principle of the helical laser drilling lens is to offer a lateral offset of the laser beam before the focusing lens. Thus, the focusing lens forms an inclined angle on the laser machining surface (Fig. 1). The focal length of the scanning lens is f_1. The image transmitting lens is f_2, and the focusing lens is f_3. Thus, the focal length of the helical laser drilling lens is f, which is expressed as follows $f=f_3\times f_1/f_2$.

In order to achieve high stability and reduce the total length, the telephoto structure and symmetry design are applied to the design of the scanning lens and image transmission lens (Fig. 2). The design specifications of the helical laser drilling lens are listed in Table 1. It is required that the diameter of the beam intersection part should be less than the minimum machining aperture to achieve the desired processing hole aperture range. The processing hole aperture range of this paper is 100–400 μm, and the depth-to-diameter ratio is 10. In order to achieve these goals, the optical system design

is carried out by using the optical design software ZEMAX. For ultrashort pulse laser, achromatic design and the best focusing performance should be considered in terms of image quality. Besides, group-velocity dispersion, thermal expansion, and damage threshold of components should all be considered in terms of system performance. Therefore, fused silica is selected as the main positive lens used in helical laser drilling lens because of its relatively high Abbe number, low heat expansion coefficient, and high damage threshold. Dense flint glass (H-ZF13, CDMG) is chosen as the material of the negative lens. The basic idea is that both lenses will compensate for their respective dispersions and cancel each other.

Results and Discussions The optical design result of the helical laser drilling lens is shown in Fig. 3, and the distribution of the focusing light field is shown in Fig. 4. The total length of the helical drilling system is 512.5 mm, which is far less than the sum of the focal length of three lenses ($f_1+f_2+f_3=950$ mm). The telephoto structure and symmetry design are helpful to reduce the total length, thus increasing the system′s stability. The spot diagrams and wave aberration results show that the on-axis and off-axis aberrations of the designed lens are almost equal, and the image quality achieves the diffraction limit. The design results show that the system can drill with a diameter of 100–400 μm, and the maximum depth-to-diameter ratio is 10∶1.

The total removal of focused ghost reflections from the optical surfaces of the helical laser drilling lens that can damage optical components is critical. Therefore, lens optimization should be conducted along with an analysis of the focused ghost positions. The main methods that eliminate the focused ghost reflections are to adjust the curvature radius and air space of lenses. The analysis of the back-focused ghost reflections of the helical laser drilling lens is shown in Fig. 6. None of the back-focused ghost reflections are inside the components or on the surfaces.

Tolerance is a critical factor that affects the performance and cost of an optical system. The tolerance of the helical laser drilling lens is analyzed in detail in this paper, as shown in Table 2. The machining and assembly tolerance analysis is put forward according to the actual condition. Analysis results show that the maximum change of spot radius (RMS) is 2.2 μm, much less than the diameter of the airy disk. The Monte Carlo simulation predicts a high-level accuracy performance for the helical laser drilling lens to be manufactured.

According to the design results, the helical laser drilling system is fabricated and assembled. An ultrashort pulse laser is used to drill micro-holes, so as to analyze the performance of the system. The results (Fig. 7) show that the helical laser drilling system can achieve high precision.

Conclusions In this paper, we have designed a helical laser drilling system based on a scanning galvanometer to meet the requirements of precise micro-hole drilling with a diameter ranging from 100 μm to a few hundred microns. Our comprehensive study has considered the essential issues in designing and optimizing the laser drilling system for high-power and high-precision applications. We have discussed helical laser drilling lens basics, principles of material selection, elimination of focused ghost reflections, and tolerance analysis. The design results show that the system can drill with a diameter ranging from 100 μm to 400 μm, and the maximum depth-to-diameter ratio is 10∶1. The experimental results show that the helical laser drilling system can achieve high precision.

Key words ultrashort pulse laser; helical drilling; micro-holes; lens; telephoto structure; tolerance analysis